

Learning Hash Codes via Hamming Distance Targets

Martin Loncaric, Bowei Liu, & Ryan Weber

Hive

{martin,bowei,ryan}@thehive.ai

Abstract

We present a powerful new loss function and training scheme for learning binary hash codes with any differentiable model and similarity function. Our loss function improves over prior methods by using log likelihood loss on top of an accurate approximation for the probability that two inputs fall within a Hamming distance target. Our novel training scheme obtains a good estimate of the true gradient by better sampling inputs and evaluating loss terms between all pairs of inputs in each minibatch. To fully leverage the resulting hashes, we use multi-indexing. We demonstrate that these techniques provide large improvements to a similarity search tasks. We report the best results to date on competitive information retrieval tasks for ImageNet and SIFT 1M, improving MAP from 73% to 84% and reducing query cost by a factor of 2-8, respectively.

1 Introduction

Many information retrieval tasks rely on searching high-dimensional datasets for results similar to a query. Recent research has flourished on these topics due to enormous growth in data volume and industry applications [19]. These problems are typically solved in either two steps by computing an embedding and then doing lookup in the embedding space, or in one step by learning a hash function. We call these three problems the data-to-embedding problem, the embedding-to-results problem, and the data-to-results problem. There exists an array of solutions for each one.

Models that solve data-to-embedding problems aim to embed the input data in a space where proximity corresponds to similarity. The most commonly chosen embedding space is \mathbb{R}^n , in order to leverage lookup methods that assume Euclidean distance. Recent methods employ neural network architectures for embeddings in specific domains, such as facial recognition and sentiment analysis [18, 16].

Once the data-to-embedding problem is solved, numerous embedding-to-results strategies exist for similarity search in a metric space. For this step, the main challenge is achieving high recall with low query cost. Exact k -nearest neighbors (KNN) algorithms achieve 100% recall, finding the k closest items to the query in the dataset, but they can be prohibitively slow. Brute force algorithms that compare distance to every other element of the dataset are often the most viable KNN methods, even with large datasets. Recent research has enabled exact KNN on surprisingly large datasets with low latency [11]. However, the compute resources required are still large. Alternatives exist that can reduce query costs in some cases, but increase insertion time. For instance, k -d trees require $O(\log N)$ search time on average with a high constant, but also require $O(\log N)$ insertion time on average.

Approximate nearest neighbors algorithms solve the embedding-to-results problem by finding results that are likely, but not guaranteed to be among the k closest. Similarly, approximate near-neighbor algorithms aim to find most of the results that fall within a specific distance of the query's embedding. These tasks (ANN) are generally achieved by hashing the query embedding, then looking up and comparing results under hashes close to that hash. Approximate methods can be highly advantageous by providing orders of magnitude faster queries with constant insertion time. Locality-sensitive hashing (LSH) is one such method that works by generating multiple, randomly-chosen hash

functions for each input. Each element of the dataset is inserted into multiple hash tables, one for each hash function. Queries can then be made by checking all hash tables for similar results. Another approach is quantization, which solves ANN problems by partitioning the space of inputs into buckets. Each element of the dataset is inserted into its bucket, and queries are made by selecting from multiple buckets close to the query.

Data-to-results methods determine similarity between inputs and provide an efficient lookup mechanism in one step. These methods directly compute a hash for each input, showing promise of simplicity and efficiency. Additionally, machine learning methods in this category train end-to-end, by which they can reduce inefficiencies in the embedding step. There has been a great deal of recent research into these methods in topics such as content-based image retrieval (CBIR). In other topics such as automated scene matching, hand-chosen hash functions are common [1]. But despite recent focus, data-to-results methods have had mixed results in comparison to data-to-embedding methods paired with embedding-to-results lookup [20, 12].

We assert the main reason data-to-results methods have sometimes underperformed is that training methods have not adequately expressed the model’s loss. Our proposed approach trains neural networks to produce binary hash codes for fast retrieval of results within a Hamming distance target. These hash codes can be efficiently queried within the same Hamming distance by multi-indexing [17].

1.1 Related Work

Additional context in quantization and learning to hash is important to our work. Quantization is considered state-of-the-art in ANN tasks [20]. There are many quantization approaches, but two are particularly noteworthy: iterative quantization (ITQ) [5] and product quantization (PQ) [9]. Iterative quantization learns to produce binary hashes by first reducing dimensionality and then minimizing a *quantization loss* term, a measure of the amount of information lost by quantizing. ITQ uses principal component analysis for dimensionality reduction and $\|\text{sgn}(v) - v\|_2$ for a quantization loss term, where v is the pre-binarized output and $\text{sgn}(v)$ is the quantized hash. It then minimizes quantization loss by alternately updating an offset and then a rotation matrix for the embedding. PQ is a generally more powerful quantization method that splits the embedding space \mathbb{R}^n into $\mathbb{R}^{n/M} \times \mathbb{R}^{n/M} \times \dots \mathbb{R}^{n/M}$. A k -means algorithm is run on the embedding constrained to each $\mathbb{R}^{n/M}$ subspace, giving k Voronoi cells in each subspace for a total of k^m hash buckets.

Recent methods that learn to hash end-to-end draw from a few families of loss terms to train binary codes [20]. These include terms for supervised softmax cross entropy between codes [8], supervised Euclidean distance between codes [13], and quantization loss terms [22]. Softmax cross entropy and Euclidean distance losses assume that Hamming distance corresponds to Euclidean distance in the pre-binarized outputs. Some papers try to enforce that assumption in a few different ways. For instance, quantization loss terms aim to make that assumption more true by penalizing networks for producing outputs far from ± 1 . Alternative methods to force outputs close to ± 1 exist, such as HashNet, which gradually sharpens sigmoid functions on the pre-binarized outputs. Another family of methods first learns a target hash code for each class, then minimizes distance between each embedding and its target hash code [21, 15].

We observed four main shortcomings of existing methods that learn to hash end-to-end. First, cross entropy and Euclidean distance between pre-binarized outputs does not correspond to Hamming distance under almost any circumstances. Second, quantization loss and learning by continuation cause gradients to shrink during training, dissuading the model from changing the sign of any output. Third, methods using target hash codes are limited to classification tasks, and have no obvious extension to applications with non-transitive similarity. Finally, various multi-step training methods, including target hash codes, forfeit the benefit of training end-to-end.

1.2 Multi-indexing

Multi-indexing enables search within a Hamming radius r by splitting an n -bit binary hash into m substrings of length n/m [17]. Technically, it is possible to use any $m \in \{1, \dots, r + 1\}$, but in most practical scenarios the best choice is $m = r + 1$. We consider only this case¹. Each of these $r + 1$ substrings is inserted into its own reverse index, pointing back to the content (Algorithm 1). Insertion runtime is therefore proportional to $r + 1$, the number of multi-indices.

Lookup is performed by taking the union of all results for each substring, then filtering down to results within the Hamming radius r (Algorithm 2). This enables lookup within a Hamming radius of r by querying each substring in its corresponding index. Any result within r will match on at least one of the $r + 1$ substrings by pigeonhole principle.

Algorithm 1 Insertion in a multi-index system

Input: binary hash h and corresponding data D
Split h into substrings h_1, \dots, h_{r+1}
for $i = 1$ **to** $r + 1$ **do**
 Add row with key h_i and data D to the i th index
end for

Algorithm 2 Lookup in a multi-index system

Input: binary hash h
Split h into substrings h_1, \dots, h_{r+1}
Initialize empty set S_D
for $i = 1$ **to** $r + 1$ **do**
 Add exact matches for h_i in the i th index to S_D
end for
Filter results with Hamming distance greater than r out of S_D
Return S_D

With a well-distributed hash function, the average runtime of a lookup is proportional to the number of queries times the number of rows returned per query. Norouzi et al. treat the time to compare Hamming distance between codes as constant², giving us a query cost of

$$\text{cost} \sim (r + 1) \frac{N}{2^{n/(r+1)}}$$

where N is the total number of n -bit hashes in the database. Like Norouzi et al., we recommend choosing r such that $n/(r + 1) \approx \log_2 N$, providing a runtime of

$$\text{cost} \sim \frac{n}{\log_2 N}$$

We build on this technique in 2.3.

2 Method

We propose a method of Hamming distance targets (HDT) that can be used to train any differentiable, black box model to hash. We will focus on its application to deep convolutional neural nets trained

¹In scenarios with a combination of extremely large datasets, short hash codes, and large r , it is more efficient to use $m < r + 1$ substrings and make up for the missing Hamming radius with brute-force searches around each substring. However, since we are learning to hash, it makes more sense to simply choose a longer hash.

²A binary code can be treated as a long for $n \leq 64$, giving constant time to XOR bits with another code on x64 architectures. Summing the bits is $O(n)$, but small compared to the practical cost of retrieving a result.

using stochastic gradient descent. Our loss function’s foundation is a statistical model relating pairs of embeddings to Hamming distances.

2.1 Loss Function

2.1.1 Motivation

Let $\mathbf{y}(\mathbf{x}) = (y_1(\mathbf{x}), \dots, y_n(\mathbf{x}))$ be the model’s embedding for an input \mathbf{x} , and let \mathcal{X} be the distribution of inputs to consider. We motivate our loss function with the following assumptions:

- If $\mathbf{x} \sim \mathcal{X}$ is a random input, then $y_i(x) \sim \mathcal{N}(0, 1)$. We partially enforce this assumption via batch normalization of y_i with mean 0 and variance 1.
- y_i is independent of other y_j .

Let $\mathbf{z}(\mathbf{x}) = \mathbf{y}(\mathbf{x}) / \|\mathbf{y}(\mathbf{x})\|_2$ be the L^2 -normalized output vector. Since $\mathbf{y}(\mathbf{x})$ is a vector of n independent random normal variables, $\mathbf{z}(\mathbf{x})$ is a random variable distributed uniformly on the hypersphere.

This L^2 -normalization is the same as SphereNorm [14] and similar to Riemannian Batch Normalization [3]. Liu et al. posed the question of why this technique works better in conjunction with batch norm than either approach alone, and our work bridges that gap. An L^2 -normalized vector of IID random normal variables forms a uniform distribution on a hypersphere, whereas most other distributions would not. An uneven distribution would limit the regions on the hypersphere where learning can happen and leave room for internal covariate shift toward different, unknown regions of the hypersphere.

To avoid the assumption that Euclidean distance translates to Hamming distance, we further study the distribution of Hamming distance given these L^2 -normalized vectors. We craft a good approximation for the probability that two bits match, given two uniformly random points $\mathbf{z}^i, \mathbf{z}^j$ on the hypersphere, conditioned on the angle θ between them.

We know that $\mathbf{z}^i \cdot \mathbf{z}^j = \cos(\theta)$, so the arc length of the path on the unit hypersphere between them is $\arccos(\mathbf{z}^i \cdot \mathbf{z}^j)$. A half loop around the unit hypersphere would cross each of the n axis hyperplanes (i.e. $z_k = 0$) once, so a randomly positioned arc of length θ crosses $n\theta/\pi$ axis hyperplanes on average (Figure 1). Each axis hyperplane crossed corresponds to a bit flipped, so the probability that a random bit differs between these vectors is

$$P_{ij} = \frac{\arccos(\mathbf{z}^i \cdot \mathbf{z}^j)}{\pi}$$

Given this exact probability, we estimate the distribution of Hamming distance between $\text{sgn}(\mathbf{y}^i)$ and $\text{sgn}(\mathbf{y}^j)$ by making the approximation that each bit position between the two vectors differs independently from the others with probability P_{ij} . Therefore, the probability of Hamming distance being within r is approximately $F(r; n, P_{ij})$ where F is the binomial CDF.

This approximation proves to be very close for large n (Figure 2.1.1).

Prior hashing research has made inroads with a similar observation, but applied it in the limited context of choosing vectors to project an embedding onto for binarization [10]. We apply this idea directly in network training.

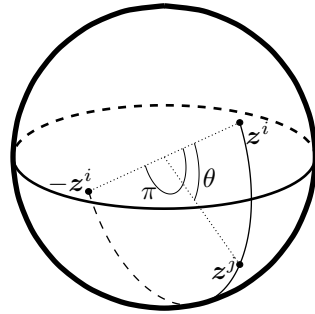


Figure 1: An arc of length θ on the unit hypersphere starting from a random point in a random direction has probability θ/π for the sign of a particular component to change along its course. In the 3D example above, crossing the great circle implies that the sign of one component differs between \mathbf{z}^i and \mathbf{z}^j .

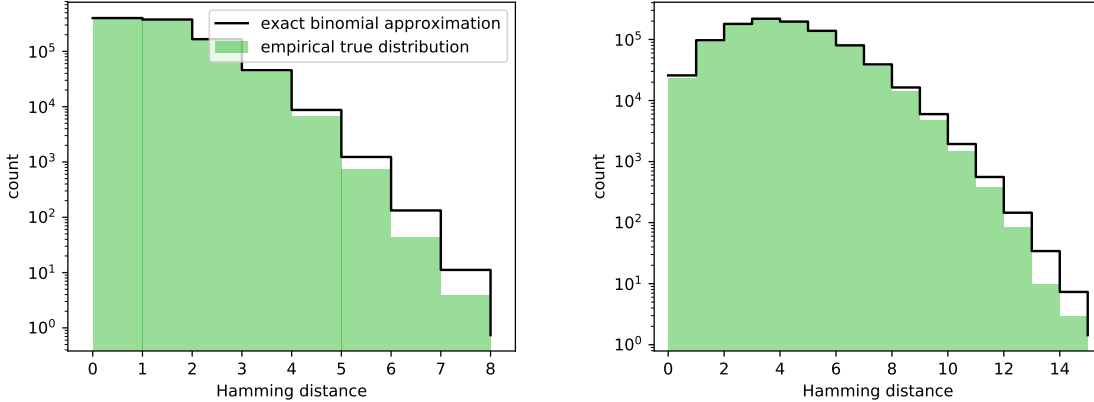


Figure 2: The empirical distribution and our binomial approximation of Hamming distance for two uniformly random vectors on the n -hypersphere, conditioned on being separated by an angle $\theta = 15^\circ$. From left to right, $n = 16, 64$. Each empirical distribution was calculated from the results of 10^6 trials.

2.1.2 Formulation

With batch size b , let $\mathbf{Y} = (\mathbf{y}^1, \dots, \mathbf{y}^b)^T$ be our batch-normalized logit layer for a batch of inputs $(\mathbf{x}^1, \dots, \mathbf{x}^b)$ and $\mathbf{Z} = (\mathbf{z}^1, \dots, \mathbf{z}^b)^T$ be the $b \times n$ L^2 -row-normalized version of \mathbf{Y} ; that is, $\mathbf{z}^i = \mathbf{y}^i / \|\mathbf{y}^i\|_2$. Let $\mathbf{P} = \frac{\arccos(\mathbf{Z}^T \mathbf{Z})}{\pi}$. Let \mathbf{w} be the vector of all our model’s learnable weights. Let \mathbf{S} be a $b \times b$ similarity matrix such that $S_{ij} = 1$ if inputs \mathbf{x}^i and \mathbf{x}^j are similar and 0 otherwise. Define \circ to be the Hammand product, or pointwise multiplication.

Our loss function is

$$J = -J_1 - \lambda J_2 + \lambda_w J_3$$

with

- $J_1 = \text{Avg}[\mathbf{S} \circ \log F(r; n, \mathbf{P})]$, the average log likelihood of each similar pair of inputs to be within Hamming distance r .
- $J_2 = \text{Avg}[(1 - \mathbf{S}) \circ \log F(n - r - 1; n, 1 - \mathbf{P})]$, the average log likelihood of each dissimilar pair of inputs to be outside Hamming distance r .
- $J_3 = \|\mathbf{w}\|_2^2$, a regularization term on the model’s learnable weights to minimize overfitting.

Note that terms J_1 and J_2 , work on all pairwise combinations of images in the batch, providing us with a very accurate estimate of the true gradient.

While most machine learning frameworks do not currently have a binomial CDF operation, many (e.g., Tensorflow and Torch) support a differentiable operation for a beta distribution’s CDF. This can be used instead via the well-known relation between the binomial CDF and the beta CDF I :

$$F(r; n, p) = I(p; n - r, r + 1)$$

For values of p that are too low, this quantity underflows floating point numbers. This issue can be addressed by a linear extrapolation of log likelihood for $p < p_0$. An exact formula exists, but a simpler approximation suffices, using the fact that $I(p; \alpha, \beta) \propto p^\alpha$ for small p :

$$\log(F(r; n, p)) \approx \begin{cases} \log(I(p; n - r, r + 1)), & p \geq p_0 \\ \log(I(p_0; n - r, r + 1)) + \frac{n-r}{p_0} (p - p_0), & p < p_0 \end{cases}$$

2.2 Training Scheme

We construct training batches in a way that ensures every input has another input in the batch it is similar to. Specifically, each batch is composed of groups of g inputs, where each group has one randomly selected marker input and $g - 1$ random inputs similar to the marker. We then choose b/g random groups to form. During training, similarity between inputs is determined dynamically, such that if two inputs from different groups happen to be similar, they are treated as such.

This method ensures that each loss term is well-defined, since there will be both similar and dissimilar inputs in each batch. Additionally, it provides a better estimate of the true gradient by balancing the huge class of dissimilar inputs with the small class of similar inputs.

2.3 Multi-indexing with Embeddings

For additional recall on ANN tasks, we store our model’s embedding in each row of the multi-index. We use this to rank results better, returning the closest l of them to the query embedding. This adds to query cost, since evaluating the Euclidean distance between the query’s embedding scales with the hash size n and obtaining the top l elements is $O(\log l)$ per result. The heightened query cost allows us to compare query cost against quantization methods, which do the same ranking of final results by embedding distance. When using embeddings to better rank results in this way, we call our method HDT-E.

3 Results

3.1 ImageNet

We compared HDT against reported numbers for other machine learning approaches to similar image retrieval on ImageNet. We followed the same methodology as Cao et al., using the same training and test sets drawn from 100 ImageNet classes and starting from a pre-trained Resnet V2 50 [6] ImageNet checkpoint accepting 224×224 images. Fine tuning each model took 5 hours on a single Titan Xp GPU. Following convention, we computed mean average precision (MAP) for the first 1000 results by Hamming distance as our evaluation criterion. We also study our model’s precision and recall at different Hamming distances (Figure 3.1).

We highlight 5 comparator models: DBR-v3 [15], HashNet [2], Deep hashing network for efficient similarity retrieval (DHN) [23], Iterative Quantization (ITQ) [5], and LSH [4]. DBR-v3 learns by first choosing a target hash code for each class to maximize Hamming distance between other target hash codes, then minimizing distance between each image’s embedding and target hash code. To the best of our knowledge, it has the highest reported MAP on the ImageNet image retrieval task until this work. HashNet trains a neural network to hash with a supervised cross entropy loss function by gradually sharpening a sigmoid function of its last layer until the outputs are all close to ± 1 . DHN similarly trains a neural network with supervised cross entropy loss, but with an added binarization loss term to coerce outputs close to ± 1 instead of sharpening a sigmoid. Using $\lambda = 2000$ and $r = 2$, our method achieved 81.2-83.8% MAP for hash bit lengths from 16 to 64 (Table 1), a 4.3-10.5% absolute improvement over the next best method.

Most interestingly, HDT performed better on shorter bit lengths. A shorter hash should be strictly worse, since it can be padded with constant bits to a longer hash. Our result may reflect a capacity for the model to overfit slightly with larger bit lengths, an increased difficulty to train a larger model, or a need to better tune parameters. In any case, the clear implication is that 16 bits are enough to encode 100 ImageNet classes.

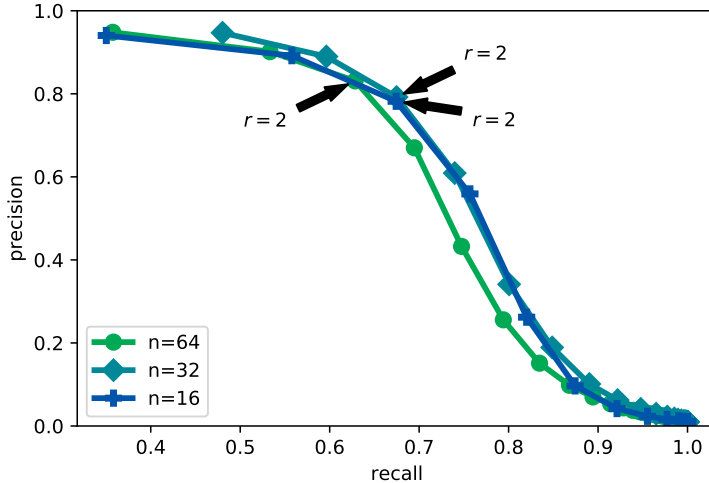


Figure 3: Our model’s precision and recall at different hash lengths for chosen Hamming radii. Note that even at a Hamming radius of 0, all models achieve roughly 40% recall.

Table 1: ImageNet MAP@1000. Other models’ performances are the best reported performances in [15] and [2].

Model	16 Bits	32 Bits	64 Bits
HDT	83.8%	82.2%	81.2%
DBR-v3	73.3%	76.1%	76.9%
HashNet	50.6%	63.1%	68.4%
DHN	31.1%	47.2%	57.3%
ITQ	32.3%	46.2%	55.2%
LSH	10.1%	23.5%	36.0%

3.2 SIFT 1M

We compared HDT against the state-of-the-art embedding-to-results method of Product Quantization on the SIFT 1M dataset, which consists of 10^6 dataset vectors, 10^5 training vectors, and 10^4 query vectors in \mathbb{R}^{128} .

We trained HDT from scratch using a simple 3-layer Densenet [7] with 256 relu-activated batch-normalized units per layer. During training, we defined input x^i to be similar to x^j if x^j is among the 10 nearest neighbors to x^i . Training each model took 75 minutes on a single Geforce 1080 GPU. We compared the recall-query cost tradeoff at different values of n , r , and λ (Table 2). We used the standard recall metric for this dataset of recall@100, where recall@ k is the proportion of queries whose single nearest neighbor is in the top k results.

HDT-E defied even our expectations by providing higher recall than reported numbers for PQ while requiring fewer distance comparisons (Figure 3.2). This implies that even on embedding-to-result tasks, HDT-E can be implemented to provide better results than PQ with faster query speeds. The improvement is particularly great in the high-recall regime. Notably, HDT-E gets 78.1% recall with an average of 12,709 distance comparisons, whereas PQ gets only 74.4% recall with 101,158 comparisons.

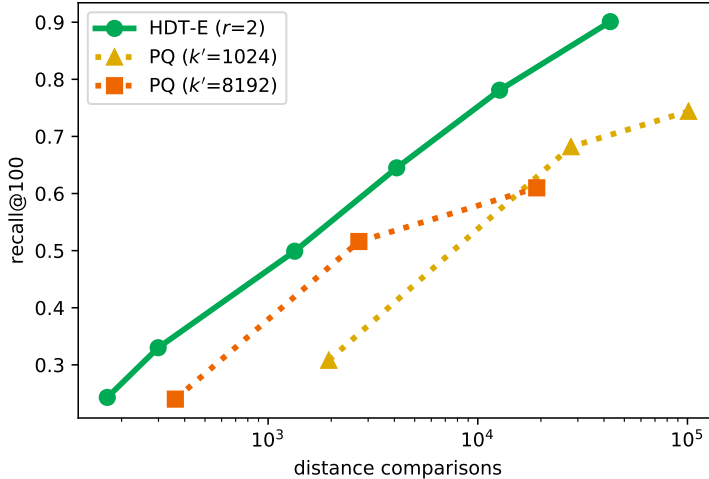


Figure 4: Comparison of HDT-E and PQ 64-bit codes. Metrics used are SIFT 1M recall@100 vs. number of distance comparisons, a measure of query cost. PQ curves are sampled at different parameters for $w \in \{1, 8, 64\}$, the number of centroids whose elements to check against the query. HDT curves are sampled for $\lambda \in \{30000, 10000, 3000, 1000, 300, 100\}$, the loss ratio for false positives.

Table 2: HDT-E SIFT 1M average recall and average number of distance comparisons made with at different values of bits per hash (n), Hamming distance target and Hamming threshold (r), and loss ratio for false positives (λ).

n	r	$\lambda = 100$	$\lambda = 300$	$\lambda = 1000$
16	0	32.4%, 1463	20.6%, 366	12.0%, 80.6
32	1	59.4%, 4984	42.0%, 1324	26.5%, 247
64	2	90.1%, 42851	78.1%, 12709	64.5%, 4105

4 Discussion

Our novel method of Hamming distance targets vastly improved recall and query speed in competitive benchmarks for both data-to-results tasks and embedding-to-results tasks. HDT is also general enough to use any differentiable model and similarity criterion, with applications in image, video, audio, and text retrieval.

We developed a sound statistical model as the foundation of HDT’s loss function. We also shed light on why L^2 -normalization of layer outputs improves learning in conjunction with batch norm. For future study, we are interested in better understanding the theoretical distribution of Hamming distances between points on a sphere separated by a fixed angle.

References

- [1] Aasif Ansari and Muzammil Mohammed. Content based video retrieval systems - methods, techniques, trends and challenges. In *International Journal of Computer Applications*, volume 112(7), 2015.

- [2] Zhangjie Cao, Mingsheng Long, and Philip S. Yu. Hashnet: Deep learning to hash by continuation. *arXiv preprint arXiv:1702.00758 [cs.CV]*, 2017.
- [3] Minhyung Cho and Jaehyung Lee. Riemannian approach to batch normalization. In *Advances in Neural Information Processing Systems 30 (NIPS 2017) pre-proceedings*, 2017.
- [4] Aristrides Gionis, Piotr Indyk, and Rajeev Motwani. Similarity search in high dimensions via hashing. *VLDB*, pages 518–529, 99.
- [5] Yunchao Gong and Svetlana Lazebnik. Iterative quantization: A procrustean approach to learning binary codes. *IEEE Transactions on Pattern Analysis and Machine Intelligence*, 35(12):2916–2929, 2013.
- [6] Kaiming He, Xiangyu Zhang, Shaoqing Ren, and Jian Sun. Identity mappings in deep residual networks. In *ECCV*, 2016.
- [7] G. Huang, Z. Liu, L. v. d. Maaten, and K. Q. Weinberger. Densely connected convolutional networks. In *2017 IEEE Conference on Computer Vision and Pattern Recognition (CVPR)*, pages 2261–2269, July 2017.
- [8] Himalaya Jain, Joaquin Zepeda, Patrick Perez, and Remi Gribonval. Subic: A supervised, structured binary code for image search. In *The IEEE International Conference on Computer Vision (ICCV)*, Oct 2017.
- [9] Hervé Jégou, Matthijs Douze, and Cordelia Schmid. Product quantization for nearest neighbor search. *TPAMI*, 33, 2011.
- [10] Jianqiu Ji, Jianmin Li, Shuicheng Yan, Bo Zhang, and Qi Tian. Super-bit locality-sensitive hashing. In *Conference on Neural Information Processing Systems*, pages 108–116, 2012.
- [11] Jeff Johnson, Matthijs Douze, and Hervé Jégou. Billion-scale similarity search with gpus. *arXiv preprint arXiv:1702.08734 [cs.CV]*, 2017.
- [12] Benjamin Klein and Lior Wolf. In defense of product quantization. *arXiv preprint arXiv:1711.08589 [cs.CV]*, 2017.
- [13] H. Liu, R. Wang, S. Shan, and X. Chen. Deep supervised hashing for fast image retrieval. In *2016 IEEE Conference on Computer Vision and Pattern Recognition (CVPR)*, pages 2064–2072, 2016.
- [14] Weiyang Liu, Yan-Ming Zhang, Xingguo Li, Zhiding Yu, Bo Dai, Tuo Zhao, and Le Song. Deep hyperspherical learning. In *Advances in Neural Information Processing Systems 30 (NIPS 2017) pre-proceedings*, 2017.
- [15] Xuchao Lu, Li Song, Rong Xie, Xiaokang Yang, and Wenjun Zhang. Deep binary representation for efficient image retrieval. *Advances in Multimedia*, 2017.
- [16] Tomas Mikolov, Ilya Sutskever, Kai Chen, Greg S Corrado, and Jeff Dean. Distributed representations of words and phrases and their compositionality. In *Advances in Neural Information Processing Systems 26*, pages 3111–3119, 2013.
- [17] Mohammad Norouzi, Ali Punjani, and David J. Fleet. Fast search in hamming space with multi-index hashing. In *IEEE Conference on Computer Vision and Pattern Recognition*, pages 3108–3115, 2012.
- [18] F. Schroff, D. Kalenichenko, and J. Philbin. Facenet: A unified embedding for face recognition and clustering. In *2015 IEEE Conference on Computer Vision and Pattern Recognition (CVPR)*, pages 815–823, June 2015.

- [19] J. Wang, W. Liu, S. Kumar, and S. F. Chang. Learning to hash for indexing big data: A survey. In *IEEE Transactions on Pattern Analysis and Machine Intelligence*, volume 104(1), pages 34–57, 2016.
- [20] J. Wang, T. Zhang, j. song, N. Sebe, and H. T. Shen. A survey on learning to hash. *IEEE Transactions on Pattern Analysis and Machine Intelligence*, 40(4):769–790, April 2018.
- [21] Rongkai Xia, Yan Pan, Hanjiang Lai, Cong Liu, and Shuicheng Yan. Supervised hashing for image retrieval via image representation learning. In *AAAI Conference on Artificial Intelligence*, 2014.
- [22] Yuefu Zhou, Shanshan Huang, Ya Zhang, and Yanfeng Wang. Deep hashing with triplet quantization loss. *arXiv preprint arXiv:1710.11445 [cs.CV]*, 2017.
- [23] Han Zhu, Mingsheng Long, Jianmin Wang, and Yue Cao. Deep hashing network for efficient similarity retrieval. *AAAI*, 2016.